agronomy

MDPI

Article

Sustainable Management of Anaerobic Digestate: From Biogas Plant to Full-Scale Cultivation of *Pleurotus ostreatus*

Veronica Zuffi [1,*], Federico Puliga [1], Alessandra Zambonelli [1], Lorenzo Trincone [1], Santiago Sanchez-Cortes [2] and Ornella Francioso [1]

[1] Department of Agricultural and Food Sciences, University of Bologna, Viale G. Fanin 40-50, 40127 Bologna, Italy; federico.puliga2@unibo.it (F.P.); alessandr.zambonelli@unibo.it (A.Z.); lorenzo.trincone@studio.unibo.it (L.T.); ornella.francioso@unibo.it (O.F.)

[2] Instituto de Estructura de la Materia, Consejo Superior de Investigaciones Cientificas (IEM-CSIC), Serrano, 121, E-28006 Madrid, Spain; s.sanchez.cortes@csic.es

* Correspondence: veronica.zuffi3@unibo.it

Abstract: In the last decades, the number of studies about the valorization of agricultural by-products has strongly increased due to the growing focus on the circular economy. In this context, mushroom cultivation is raising attention for its nutritional properties and adaptability to different growing conditions. The goal of this project is, therefore, to create a link between two production chains, valorizing the solid anaerobic digestate fraction from the biogas plant as a potential substrate for *Pleurotus ostreatus* full-scale cultivation. A preliminary in vitro trial shows that the mycelia can colonize at the same rate in both the conventional substrate, which was wheat straw added with sunflower cake and the experimental ones supplemented with corn digestate. The most important and innovative part of the work was full-scale cultivation. Quantitative analyses demonstrate that *P. ostreatus* is capable of growing on the conventional substrate as well as on the substrate containing 15% of digestate without reducing the mushroom harvest. Even better, digestate seems to stimulate a precocious and more homogeneous production. Chemical and spectroscopic analyses on the fruiting bodies confirm the results; in fact, mushrooms show a comparable structural composition, highlighted with FTIR and SERS spectroscopic evaluations. Moreover, the nutrient content did not change due to the addition of digestate. These promising results demonstrate that anaerobic digestate can become a resource for *P. ostreatus* cultivation without production losses and maintaining the same qualitative characteristics.

Keywords: by-products; agro-waste; biomass valorization; circular economy; mushroom cultivation; SERS spectroscopy; ATR-FTIR

Citation: Zuffi, V.; Puliga, F.; Zambonelli, A.; Trincone, L.; Sanchez-Cortes, S.; Francioso, O. Sustainable Management of Anaerobic Digestate: From Biogas Plant to Full-Scale Cultivation of *Pleurotus ostreatus*. *Agronomy* **2023**, *13*, 950. https://doi.org/10.3390/agronomy13040950

Academic Editor: Gerardo Fernández Barbero

Received: 22 February 2023
Revised: 20 March 2023
Accepted: 21 March 2023
Published: 23 March 2023

1. Introduction

In recent years the nutritional value and the sustainability of the food chain are becoming increasingly relevant; consumers search for more healthy food whose production has a low environmental footprint in terms of greenhouse gasses emissions (GHG) and biodiversity preservation [1]. In this context, mushrooms have received great attention for their medicinal and nutritional properties; they are, indeed, rich in protein, essential amino acids, vitamins, and fiber and, at the same time, low in calories and fat [2–4]. Moreover, their cultivation is not so impactful, considering the energy input, the land usage, and the growth time required [5]. For these reasons, mushroom production has strongly increased in the last decades, reaching a global production of approximately 9 million tons in 2018 [6], and it is expected to continue growing in the next years [7].

Nowadays, to effectively face climate change, more and more industries have to re-evaluate their production processes. In accordance with the above, mushroom cultivation can be easily placed in the context of a circular economy. Placing the focus on the growing substrates, waste matrices different from those commonly used have been tested with

the purpose of reducing costs in the meantime valorizing by-products from other supply chains [8,9].

Agriculture is one of the main activities that produce large volumes of by-products every year. Most of these residues remain underutilized and usually are disposed of in landfills or burned, becoming a risk to the environment [10,11]. In recent years, great attention has been given to innovative agricultural or correlated activities [12] commonly considered sustainable, such as the biogas industry [13]. The European Commission, in the REPowerEU plan, calls for a rapid speed-up of renewable energy that includes 35 billion biomethane by 2030 and a new biomethane industry partnership to "support the achievement of the target and set the stage for further increase towards 2050" [14]. Although its potential as a renewable resource, the sustainability of its production also depends on waste management, mainly represented by anaerobic digestate. It is estimated that its production reaches almost 180 million tons per year only in Europe [15]. This by-product is principally used as an amendment or fertilizer since it is rich in macro- and micro-elements and it is an important source of organic matter. However, its land spreading is strictly regulated (Nitrate Directive 91/676/ECC) to protect vulnerable areas from nitrate pollution. Other critical issues are the variability of the starting matrices as well as the degradation rate, which makes digestate not always suitable for direct usage [13,16,17]. As reported by Dahlin et al. (2015) [18], the high productivity and potential of this product without any alternative application may cripple the industry. Hence, it seems essential to research other methods to manage and valorize digestate in view of the environmental and economic sustainability of the biogas production chain.

The fungi of the genus *Pleurotus*, commonly known as oyster mushrooms, are among the most cultivated mushrooms worldwide [19]. Their adaptability to various growing conditions makes their cultivation easier compared to others. For example, they generally require a short growth time, tolerate a wide range of temperatures and chemical input, and are not often attacked by pathogens [20]. In addition, as saprotrophs, they naturally grow on waste or dead substrates for which they are primary decomposers thanks to their complex enzyme machinery (e.g., laccase, endoglucanase enzymes) [10,21]. In fact, it has been observed that many *Pleurotus* spp. can degrade macromolecules such as cellulose, hemicellulose, and lignin which are the main compounds of vegetable residues [8]. Concerning the industrial production of *Pleurotus* mushrooms, the principal matrix used is wheat straw [22]; however, diversifying the growing media may represent an economic advantage so as to create a new chain of products and support local economies, perhaps minimizing transport requirements.

Several previous works have shown that different species of *Pleurotus* are able to grow on various agro-residues, including grape pomace [2], hazelnut shells [23], banana leaves, sunflower stalk, cotton stalk, and sugar cane straw, proving their potentiality [10]. The mycelial growth of different fungi on digestate, including *Pleurotus* spp., has already been demonstrated in previous works [24,25]. Nevertheless, there is a general lack of research on the industrial application of this promising cultivation substrate.

The purpose of this study is, therefore, to explore the potential of solid anaerobic digestate as an alternative substrate for industrial-scale cultivation of mushrooms. The key point is the recycling of agricultural waste to create new products with high added value. In this perspective, a strain of *Pleurotus ostreatus* (Jacq.) P. Kumm., the most popular oyster mushroom, was grown on corn silage digestate in vitro and in vivo trials. The adaptability of full-scale cultivation was tested in an industrial mushroom company, which is also near the biogas plant, in order to minimize transport costs and sustain the local economy. To this end, the productivity, biological efficiency, and quality parameters of the mushrooms were evaluated and compared with those cultivated on a conventional substrate. Fourier transform infrared spectroscopy (FTIR) was employed to explore the substrates before and after cultivation as well as the molecular structure of the fruiting bodies. Additionally, Surface-enhanced Raman spectroscopy (SERS) was used to analyze the polysaccharides of the fruiting bodies. Actually, these methods have been successfully proven for the study

of organic material as well as for biological tissues [26–28]. Specifically, SERS is a highly sensitive vibrational technique that, thanks to the use of nanostructured metals (Au and Ag), permits a better and more rapid detection of trace amounts of molecules, including some typical fungal compounds, as previously reported by Fornasaro et al. (2021) and Puliga et al. (2022) [29–32]. The efficiency of SERS is based on the interaction between the incident light and the metal nanostructures resulting in the so-called localized surface plasmon resonance effect. This resonance leads to a strong enhancement of the Raman scattering up to 10^{14} orders of magnitude in comparison to the normal Raman spectroscopy. [33,34]. This enhancement strongly depends on the optical properties of the nanostructures provided by the metal nature, the nanoparticle size and shape, as well as on the laser excitation wavelength and the Raman cross sections of analytes [35,36].

2. Materials and Methods

2.1. Substrates

Durum wheat straw (*Triticum durum* Desf., WS) and sunflower cake (SC) were supplied by Funghitex company (Latina, Italy). The SC is added to 2–4% of the total weight of the dry straw.

Corn digestate was kindly provided by the Mascetti-Sbardella farm, which is located in Latina, Italy. The biogas plant can be defined as of compact dimension since it works with high concentrations of substrate, and it can produce around one million kWh/year of gross renewable electric energy. The plant is fed primarily with energy crops such as maize or alfa-alfa and, to a small extent, with olive pomace and horticultural wastes. The digestate for this study was obtained in January and collected as soon as it fell out of the mechanical separation and mixed for 24 h.

2.2. Mycelial Cultures and Growth Rate Evaluation

The commercial strain of *P. ostreatus* (W.H.90 from White2000) was provided by Funghitex company. One grain spawn was inoculated in each Petri dish with 20 g/L of Potato Dextrose Agar (PDA) added with 0.3 mg/mL of streptomycin sulfate. After one week, the mycelia were transferred to a new Petri dish with another antibiotic (0.3 mg/mL of chloramphenicol). The pure mycelial cultures were kept at 22 ± 1 °C in darkness and subcultured every 60 d.

To evaluate the mycelial growth on the plate, a 9 cm sterilized Petri dish was filled with the different substrates: digestate (D), wheat straw added with sunflower cake (WS + SC) as control, WS + SC 80% − D 20% (D20), WS + SC 90% − D 10% (D10). After that, plugs of 10 mm diameter were taken by 15-day-old colonies and inoculated in the center of the plates. To evaluate the growth on the plate, the substrates were previously soaked for 30 min with distilled water and brought to 70–80% humidity. An amount of almost 30 g of each substrate was transferred to a Petri dish and autoclaved at 121 °C for 1 h. Five replicates were made for each experimental sample and incubated at 22 ± 1 °C in darkness. To assess the fungal growth, we measured the diameter of the colony along two preset diametrical lines every day. The mycelium colony area (A, cm^2) was calculated assuming an elliptical shape using the following formula:

$$A = \pi \times R_1 \times R_2 \quad (1)$$

where R_1 and R_2 are the two perpendicular radii, respectively [37].

The area growth rate (AGR) was calculated through the formula:

$$AGR = \frac{(Af - Ai)}{(Tf - Ti)} \quad (2)$$

as described by Sinclair and Cantero [38], where Af and Ai are the colony area at the final growth time (Tf) and initial growth time (Ti), respectively.

2.3. Preparation of Substrates for Full-Scale Mushroom Cultivation

Full-scale cultivation was performed directly at the Funghitex farm. For the fruiting body production, two substrates were tested, WS + SC as the control and WS added with 15% of digestate (D15) as the experimental one.

For both trials (WS + SC and D15), wheat straw was previously crushed into small portions and mixed with sunflower cake pellets (4% of WS dry weight). The mix was then hydrated and stored for 12 h to drain excess water and to reach a humidity content of about 75% [39]. Subsequently, it was subjected to a first controlled aerobic fermentation; after 36 h, the substrate was amalgamated and transferred in a second fermentation tunnel, thus avoiding anaerobic conditions. The second phase was pasteurization, which is essential to prevent pathogen contamination. This process includes a first step around 72–74 °C with water vapor insufflation. Then the substrate was conditioned to 48 °C for 24 h through the addition of cool air filtered with a High Efficiency Particulate Air (HEPA) filter. The aim is to stimulate the growth of positive spontaneous Actinomycetes, which compete with other microorganisms and maintain low temperatures. After the pasteurization, the optimal sowing parameters must be reached, around 20–26 °C, 75% of humidity, and pH greater than 8.

The starting matrix was composed of sterilized millet grain inoculated with the *P. ostreatus* strain W.H.90. The cultivation bags consisted of 20 L of millet grains (11.2 kg) per ton of substrate.

For the experimental substrate (D15), the addition of a 15% digestate mixture was chosen for a dry weight of wheat straw. The choice of this percentage was made in accordance with the company based on the outcome obtained from the mycelial cultivation and with the purpose of starting testing this new compound on a full scale. The mix was then fermented and pasteurized to avoid pathogen contamination, as described in the previous section.

Bags were moved to a climate chamber for the incubation phase. The environmental conditions were maintained to optimum levels for *P. ostreatus* development (~20 °C for the colonization, ~13–15 °C for fruiting, and relative humidity 80–85%) as described by Oei (2003) [39].

2.3.1. Experimental Design

The experimental design was organized into 8 rows randomly divided into 4 control rows with WS + SC and 4 with D15. Each row consisted of 15 bags stacked in threes, for a total amount of 60 bags (Figure 1).

Figure 1. Mushroom growing room at the Funghitex company (Photo courtesy of Funghitex).

2.3.2. Mushroom Parameters

The mature fruiting bodies were collected after one month, and their fresh weight was recorded. For the dry weight, a sample of mushrooms was collected from each row and dried in a stove at 40 °C for 48 h. The fresh weight of the substrate was measured before the cultivation. The dry weight is obtained by the fresh weight divided by the coefficient 2.5 corresponding to the company's standard moisture content. This coefficient is based on a number of statistically validated measurements made previously by the company to standardize the dry weight of the bags. Biological efficiency (BE, %) was estimated as follows:

$$\text{BE} = \left(\frac{\text{Mushroom Fresh Weight}}{\text{Substrate Dry Weight}} \right) \times 100 \quad (3)$$

The precociousness (P) was calculated as the yield in the first half of harvest time divided by the yield in total harvest time and represented a measure of the yield at the mid-cycle of the production (higher values mean better P) as previously reported by Janinska et al. (2022) [40].

2.4. Chemical Analyses of Substrates and Mushrooms

Total carbon and nitrogen contents of substrates, previously finely ground by a ball mill, were carried out by an elemental analyzer (CHNS-O EA 1110 Thermo Fisher Scientific, Waltham, MA, USA). The concentration of ammonium nitrogen was performed according to APHA (1992).

Metal contents were determined in finely ground substrates and mushrooms (500–700 mg). The samples were kept in a Teflon tube with HNO_3 suprapur (Carlo Erba Reagents Srl, Milan, IT) and H_2O_2 (30%) in a microwave oven for acid digestion (Milestone, Shelton, CT, USA), according to the procedure described by Cocchi et al. (2006) [41]. After mineralization, the samples were diluted with Milli-Q® ultrapure distilled water. Each element was assayed via Inductive Coupled Plasma-Optic Emission Spectroscopy (Spectro Amatek Arcos II ICP-OES, Kleve, Germany). All analyses were performed in triplicate. The pH values were determined by a digital pH meter using a 1:2 sample-to-water ratio. Additionally, the fruiting bodies were examined for the presence of coliform bacteria according to ISO 4832 (2006) and agrochemical residues according to UNI EN 15662 (2018).

2.4.1. ATR-FTIR Spectroscopy

Different substrates before *P. ostreatus* inoculation and after 30 d of mycelial growth and fruiting bodies after full-scale cultivation were characterized by using a Bruker Tensor FTIR instrument (Bruker Optics, Ettlingen, Germany) equipped with an Attenuated Total Reflectance (ATR) accessory (Specac Quest ATR, Specac Ltd., Orpington, Kent, UK). The sampling device contained a microDiamond crystal, a single reflection with an angle of incidence of 45°, and a penetration of around 2 µm. The spectra were acquired against a pre-established background by averaging 64 scans from 4000 to 400 cm^{-1} at a 4 cm^{-1} resolution.

Grams/386 spectroscopic software (version 6.00, Galactic Industries Corporation, Salem, NH, USA) was used for spectra processing.

2.4.2. Polysaccharides Extraction

The extraction of polysaccharides from the fruiting bodies was carried out as described by Puliga et al. (2022) [30]. Briefly, the powder was immersed in an 85% ethanol solution and treated overnight. The samples follow a first centrifugation at 4500× *g* for 15 min and then an extraction in distilled water (25 mL for each g of precipitate) at 70 °C for 140 min. The second centrifugation was carried out for 10 min at 4500× *g*. The supernatant was deproteinized using a Sevag reagent (butanol:chloroform, 1:4 *v*/*v*) and centrifuged at 4500× *g* for 10 min. The precipitation of crude polysaccharides was obtained by removing the upper layer of the centrifugate and mixing that with a four-fold volume of absolute

ethanol for 12 h at 4 °C. Finally, another centrifugation was conducted, and the precipitate was washed with ethanol and acetone, and lyophilized.

2.4.3. SERS Analyses

To carry out SERS analyses, silver nanoparticles were prepared as previously described by Leopold and Lendl (2003) [42]. For sample preparation, small portions of dry fruiting bodies, supplemented with 1 mL of Milli-Q® ultrapure distilled water, were soaked for 24 h into a 1.5 mL microtube, centrifuged at 11,000 × *g* for 10 min and, in the end, all the water was removed. The wet portions were next deposited on a microscope slide glass and coated with 5 µL of a concentrated Ag-NPs suspension. This last was previously obtained by centrifugation of 500 µL and successive redispersion to 10% of the initial volume, as described by Puliga et al. (2022) [30]. Prior to SERS analyses, the resulting samples were dried at room temperature.

SERS measurements were performed by using the portable spectrometer Raman Virsa™ (Renishaw, Wotton-under-Edge, UK) with a 785 nm laser. Prior to the analysis, a calibration of the instrument was needed by using a Si reference sample. A 50× objective long focal lens with the laser power set at 2 mW and an integration time of 10 s was employed to analyze the mushroom fragments.

2.5. Statistical Analyses

Statistical analyses were carried out using the RStudio graphical interface for the R software environment v.4.2.1 (R Foundation, Vienna, Austria). Preliminary tests were performed in order to evaluate the data, such as Shapiro and Levene tests. The analysis of variance (ANOVA) was used to determine the significant difference in fresh weight, AGR, and BE among different growing media. Tukey post hoc test ($p < 0.05$) was used to compare AGR means.

3. Results

3.1. Chemical and Spectroscopical Analyses of the Substrates

Table 1 provides the results obtained from the chemical analyses of the two matrices. Organic carbon content was approximately 40% in WS + SC as in D. The total amount of nitrogen was much higher in D (1.20%) as compared to WS + SC (0.48%). Further on, D appears to be rich in some macroelements such as N, P, S, and K as well, as it shows a high content in some microelements like Na, Mg, Zn, and Mn. On the other hand, the conventional substrate seems to have a similar composition in K, Cu, Zn, and Mn, whereas the amount of Ca and Fe is higher. The pH value tends to neutrality in WS + SC, while D is more alkaline, possibly due to the NH_4^+ and carbonate components.

Table 1. Chemical analyses of the conventional substrate (WS + SC) and digestate (D).

Parameters [1]	Unit	WS + SC	D
OC	% d.m.	40.15 ± 0.002	37.66 ± 0.96
N tot	% d.m.	0.48 ± 0.001	1.20 ± 0.005
NH_4^+	% d.m.	n.d.	0.27
pH		6.5	9.06
P	mg/kg	334	2417
S	mg/kg	617	1148
K	mg/kg	6328	6514
Na	mg/kg	150	1598
Ca	mg/kg	10,147	4863
Mg	mg/kg	992	1598
Fe	mg/kg	1401	595
Cu	mg/kg	7	9
Zn	mg/kg	29	47
Mn	mg/kg	53	67

[1] Abbreviations: OC—organic carbon, N tot—total nitrogen, d.m.—dry matter, n.d.—not detected. If not specified, the error value is less than 0.05%.

The ATR-FTIR spectra (1800–850 cm^{-1}) of the starting substrates are shown in Figure 2. The spectroscopic analysis of both WS + SC and D reveals a predominant peak at 1029 and 1038 cm^{-1}, respectively, which is characteristic of the polysaccharide region (cellulose and hemicellulose) for C-O and C-H group deformations [24,43].

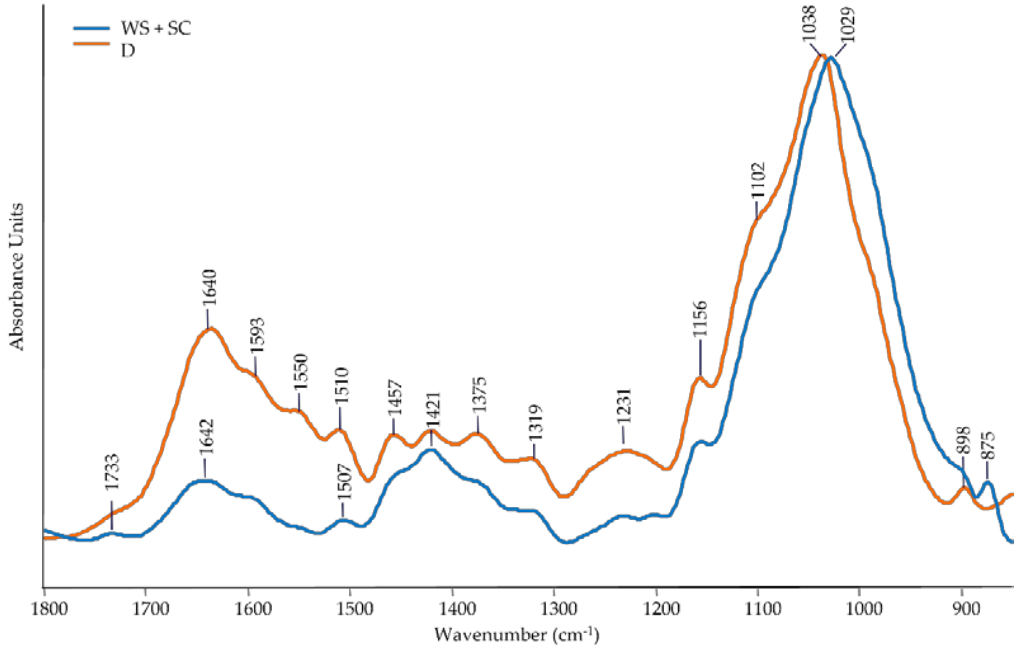

Figure 2. ATR-FTIR spectra of WS + SC (blue line) and D (orange line) before the cultivation.

In addition, connected to the structure of the polysaccharides, there are two bands at 1421 cm^{-1} and 1319 cm^{-1} assigned to CH_2 bending at C-6 of the crystalline cellulose, and a peak at 1375 cm^{-1} associated with CH_2 bending vibrations in cellulose and hemicellulose [24]. A small band at 1733 cm^{-1} is observed, probably ascribed to the C=O stretching vibration in the ester linkage connected to the hemicellulose structure [43,44]. Lastly, the peak around 898 cm^{-1}, in either WS + SC and D and that at 875 cm^{-1} in WS + SC, are related to C-H deformation in cellulose. Another fundamental compound detectable in both matrices is lignin. Although it is more evident in D, both spectra show two bands around 1590 and 1510 cm^{-1} attributed to the aromatic skeletal vibration and aromatic breathing in lignin, respectively [43]. The broad peak around 1640 cm^{-1} is possibly due to C=O stretching in conjugated ketones, water, and Amide I (proteins), while that at 1550 cm^{-1} is attributed to Amide II (proteins) [24,45].

3.2. In Vitro Mycelial Growth of P. ostreatus and ATR-FTIR of Exhausted Substrates

The in vitro mycelial growth of *P. ostreatus* on four different substrates (WS + SC, D10, D20, and D) is illustrated in Figure 3. It is apparent from the trend that the complete colonization of the plate took almost two weeks. The exponential phase in which the growth is more rapid ends around day 10 for all the tested substrates, although D seems to stimulate a faster initial development.

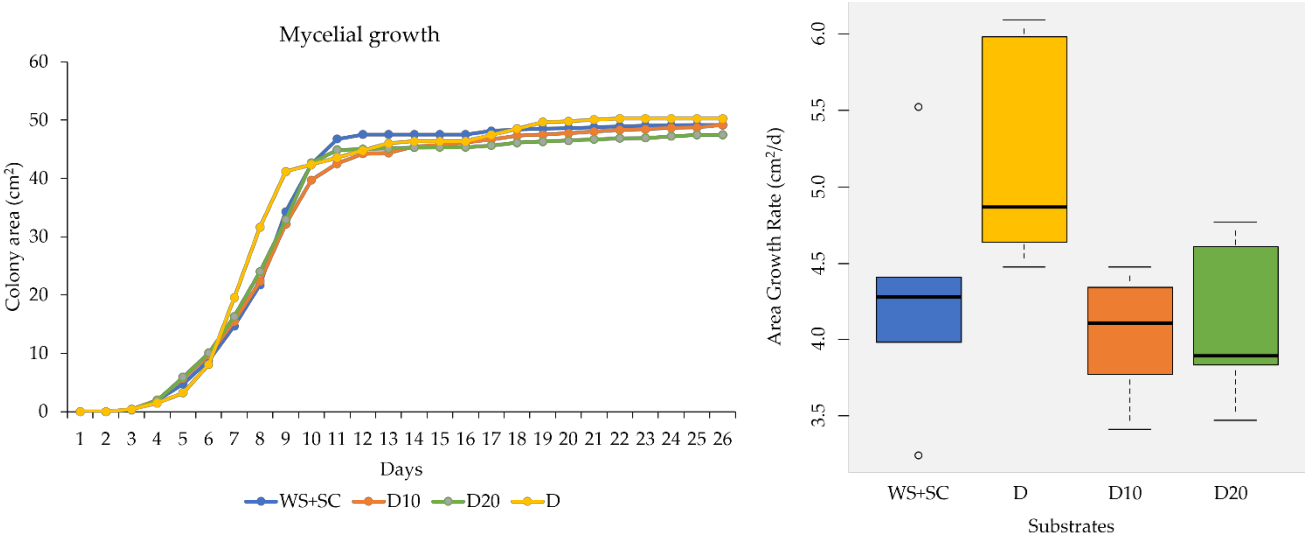

Figure 3. Mycelial growth and AGR of *P. ostreatus* in Petri dishes on WS + SC (blue), D10 (orange), D20 (green), and D (yellow). Statistical differences ($p < 0.05$) between D-D10.

To corroborate this hypothesis, an ANOVA test was performed among different AGRs calculated. From the box plot, statistical differences were observed only between D and D10. Despite this, D shows high values of AGR in some cases, up to 6 cm^2/d.

In order to evaluate changes in the molecular structure of the matrices used, the ATR-FTIR spectra after 30 d of cultivation were compared to that of the starting substrates (Figure 2). Figure 4 shows a specific spectral range, between 1800–1300 cm^{-1}, where the main differences were observed. As can be seen from Figure 4a, WS + SC exhibits consistent structural variation in this region. Specifically, the spectrum highlights a decrease of the absorption band at 1507 cm^{-1} corresponding to the aromatic skeletal vibration as well as those at 1454 and 1421 cm^{-1}, which derive from C-H bending in lignin. In addition, an important reduction in the peak at 1733 cm^{-1} may be ascribed to p-coumaric acids in the lignin structure and likewise to the ester group in hemicellulose. The enhancement of the band at 1322 cm^{-1} due to C-H bending vibration, as well as that at around 1643 cm^{-1}, assigned to C=O stretching in conjugated ketones and carboxylate in lignin, were noted. These spectral changes were previously observed by Fornito et al. (2020) [24] on the effective degradation of the substrate by *Pleurotus* spp. Specifically, the mushroom selectively degrades lignin and 'hemicellulose prior to cellulose attack.

Less structural changes emerged in D spectra, as illustrated in Figure 4b. The intensity of the band taken as a reference of lignin (1510 cm^{-1}) and amide II in proteins (1550 cm^{-1}) shortly decreased.

3.3. Full-Scale Cultivation

The bar chart in Figure 5a compares the summary statistics for the fresh weight average of the fruiting bodies harvested from the two substrates. The total yield for the conventional sample (WS + SC) was about 237.50 kg, while for the experimental one (D15) was about 249.60 kg of fruiting bodies. The ANOVA did not show any statistical differences between the fresh weight of the two groups. Furthermore, in Figure 5b, BE for each matrix is reported. Statistical analysis did not show any differences in this case as well, between the conventional matrix and the experimental one. Nevertheless, a slight increase in the fresh weight and more homogeneous results in terms of standard error can be noticed using D15.

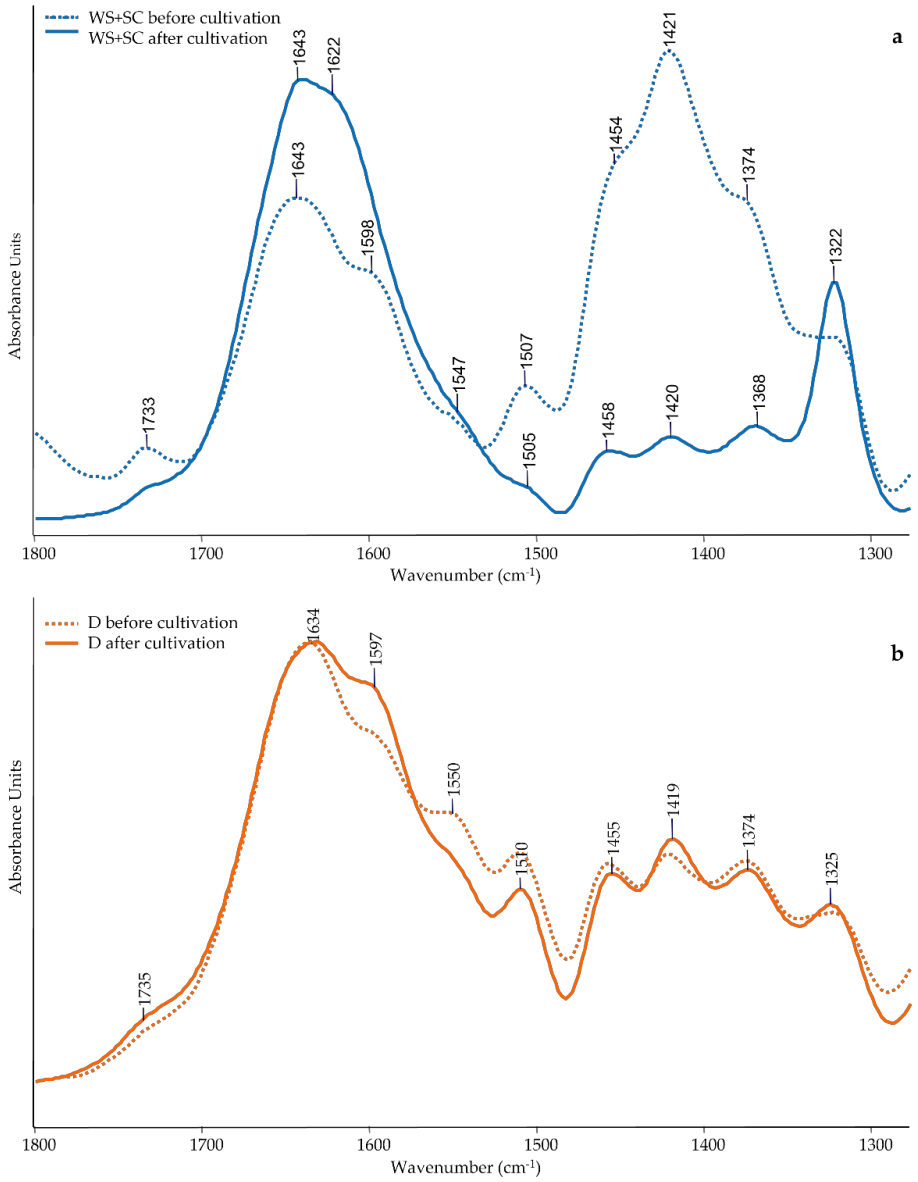

Figure 4. ATR-FTIR spectra (1800–1300 cm^{-1}) of WS + SC (**a**) and D (**b**) before the mycelial growth (dotted line) and after *P. ostreatus* mycelial growth (solid line).

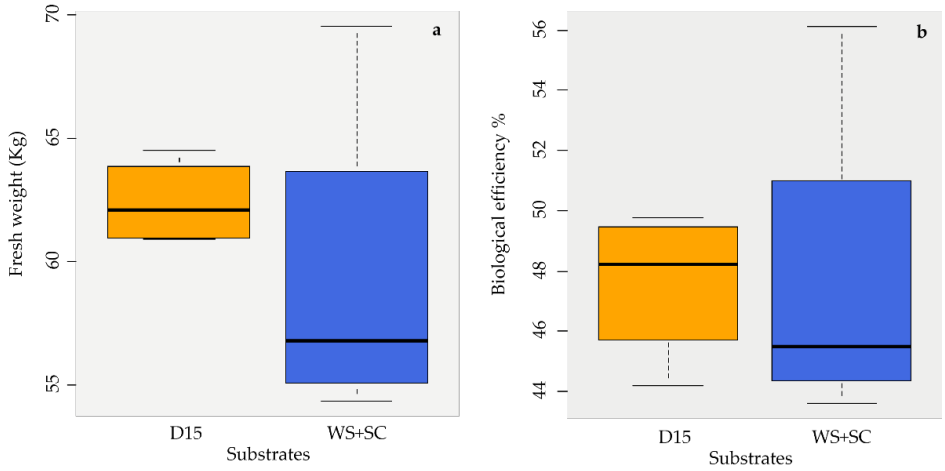

Figure 5. Fresh weight (**a**) and BE (**b**) of *P. ostreatus* grown on D15 (orange) and WS + SC (blue).

Another parameter evaluated was P during the first and second flushes. Again, as can be seen from Table 2, we found no statistical differences between D15 and the control. Nevertheless, using the experimental substrate, higher percentages were achieved in the first half of both harvesting periods as well as more homogeneous values among replicates. Figure 6 presents the trend of the daily global production of each trial through the two flushes. Especially in the first one, it is immediately evident that D stimulates the production around days 2 and 3 instead of WS + SC, whose production reaches a peak around day 5. In the second flush, the two substrates tend to have almost the same trend, with the maximum production around day 4.

Table 2. P expressed in percentage of *P. ostreatus* grown on WS + SC and D15.

Sample	First Flush			Second Flush		
	Yield 1 Half	Total Yield	P (%)	Yield 1 Half	Total Yield	P (%)
WS + SC	32.75	49.70	66%	6.00	19.85	30%
WS + SC	13.95	38.50	36%	16.10	19.30	83%
WS + SC	13.90	40.00	35%	8.20	14.35	57%
WS + SC	11.05	42.60	26%	5.60	13.20	42%
Mean	17.91 ± 9.98	42.70 ± 4.96	41%	8.98 ± 4.88	16.68 ± 3.89	53%
D15	21.20	38.00	56%	19.05	22.90	83%
D15	27.15	43.50	62%	13.40	21.00	64%
D15	24.50	40.40	61%	15.35	20.60	75%
D15	33.70	45.50	74%	12.85	17.70	73%
Mean	26.64 ± 5.30	41.85 ± 3.32	63%	15.16 ± 2.80	20.55 ± 2.15	74%

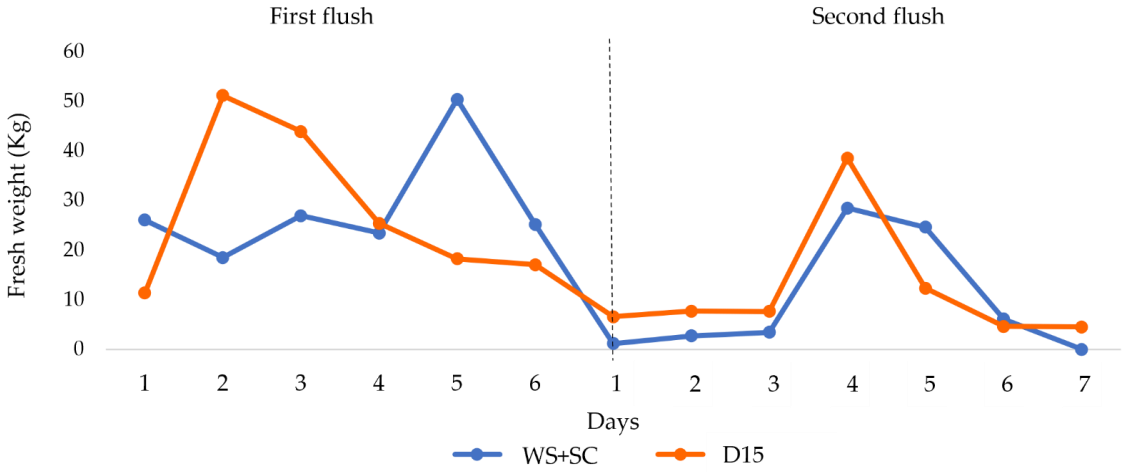

Figure 6. Yield trend of *P. ostreatus* grown on WS + SC (blue line) and D15 (orange line), expressed as total fresh weight per day in the first and second flushes.

3.4. Qualitative Evaluation of the Fruiting Bodies

3.4.1. Chemical Parameters

Table 3 shows the output of the chemical analyses of the fruiting bodies. The resulting values reveal that the nutrient composition is statistically comparable between mushrooms grown on WS + SC and those grown on the experimental substrate. The pH value was neutral and did not exhibit any changes; Fe seems to be the most abundant microelement, and its content results a little higher in those mushrooms grown in the presence of D. At that condition. Conversely, the amount of Zn undergoes a reduction. Moreover, it is important to note that nitrates and heavy metal content remain under the permitted limits in both cases. Similarly, the microbiological parameters, as well as the agrochemical residues, were under detectable levels.

Table 3. Chemical parameters of the fruiting bodies of *P. ostreatus* harvested from the conventional substrate (WS+SC) and the experimental one (D15).

Parameter	Unit	WS + SC	D15
pH		6.2 ± 0.8	6.2 ± 0.8
NO_3^-	mg/kg	<50	<50
NO_2^-	mg/kg	<50	<50
Fe	mg/kg	6.2 ± 1.5	7.4 ± 1.8
Cu	mg/kg	0.9 ± 0.3	2.0 ± 0.6
Zn	mg/kg	6.1 ± 0.5	1.0 ± 2.1
Mn	mg/kg	0.8 ± 0.3	1.2 ± 0.4
Cd	mg/kg	n.d. [1]	n.d.
Pb	mg/kg	n.d.	n.d.
Co	mg/kg	n.d.	n.d.
Ni	mg/kg	n.d.	n.d.
Total coliforms	UFC/g	<10	<10
Agrochemicals	mg/kg	n.d.	n.d.

[1] n.d.—not detected.

3.4.2. ATR-FTIR Analysis

Figure 7 illustrates the ATR-FTIR spectra of the fruiting bodies of *P. ostreatus* harvested from the two growing substrates (WS + SC and D15). Overall, no significant differences were found between mushrooms produced on WS + SC and those on the experimental matrix. In both spectra are well evident the protein bands, including Amide I at 1641 cm^{-1}, Amide II at 1544 cm^{-1}, and Amide III around 1240 cm^{-1} [23,46]; however, a slight increase can be seen in those mushrooms cultivated with the addition of digestate. Furthermore, the region around 1000 cm^{-1}, which corresponds to the polysaccharide vibration, is clearly apparent. For instance, the peak at 1146 cm^{-1}, as well as that at 1035 cm^{-1}, can be attributed to the C-O-C asymmetric stretching of glycosidic linkage and the stretching vibration of the C-O-C group, respectively [23]. The lipid component that can be found in cell membrane phospholipids, just like in the surface of the cap and stipe, can be observed at 1741 cm^{-1} and 1239 cm^{-1} due to the stretching of ester groups [47]. Along with this, the bands 1451 and 1239 cm^{-1} correspond to the aliphatic compounds.

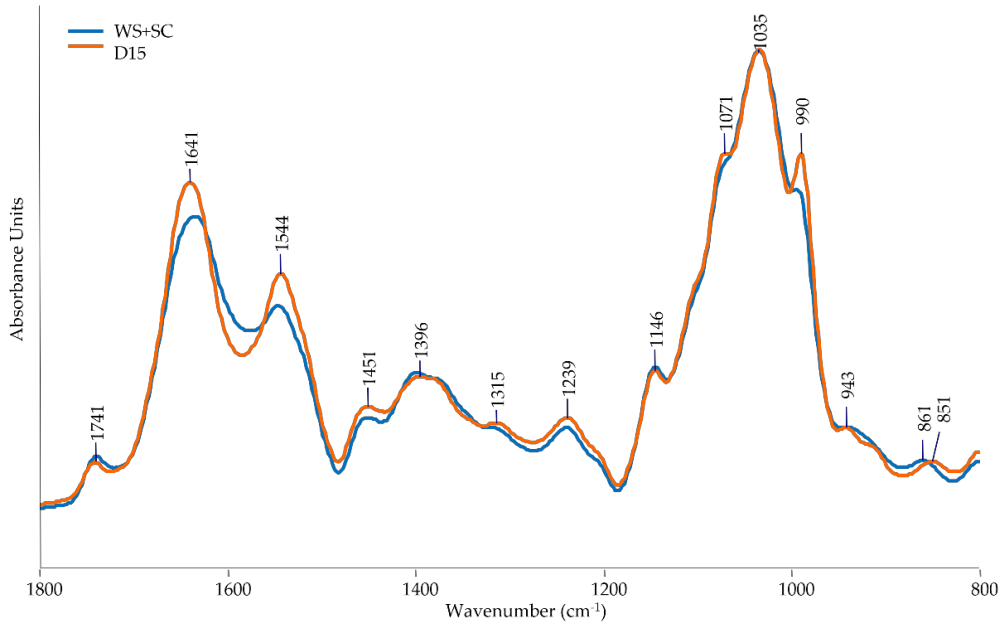

Figure 7. ATR-FTIR spectra (1800–800 cm^{-1}) of the fruiting bodies of *P. ostreatus* harvested from the two growing substrates WS + SC (blue line) and D15 (orange line).

3.4.3. SERS Analysis

SERS spectra are characterized by strong bands at 1583, 1445, 1324, and 1223 $cm^{-1,}$ which can be attributed to the imidazole-2-thione structure that forms the ergothioneine amino acid (Figure 8). The strong band seen at 486 cm^{-1} is a characteristic feature of this compound, and it was attributed to NCS bending coupled to C-S stretching from the imidazole thione ring [29]. Overall, the SERS spectral profiles of the fruiting bodies of *P. ostreatus* harvested from the two growing substrates, WS + SC and D15, are quite comparable. However, some differences can be noticed in the relative intensities of bands at 1324 and 1223 cm^{-1}, which correspond to the in-plane stretching motions of the imidazole thione ring.

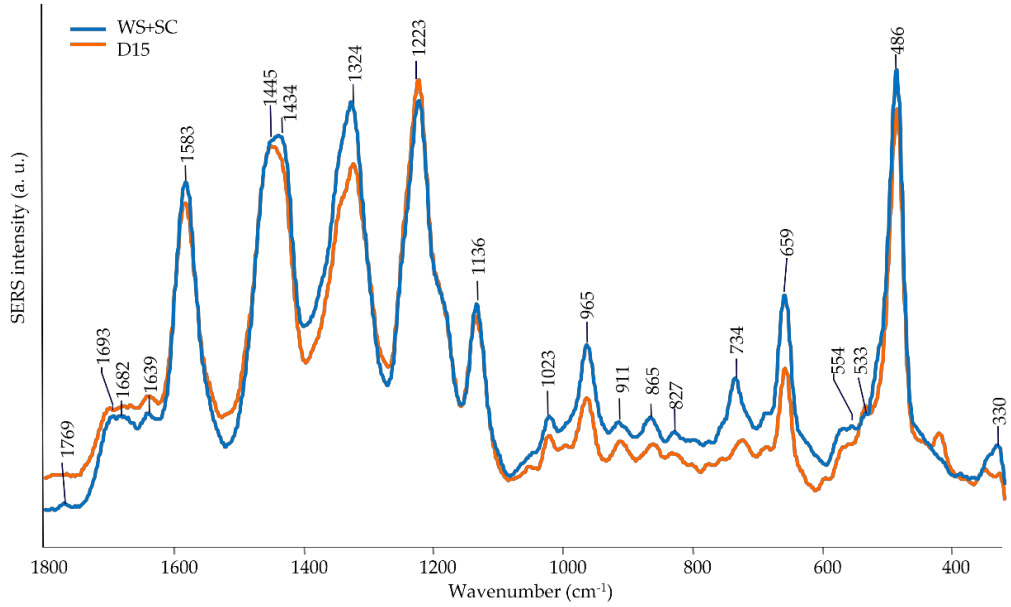

Figure 8. SERS spectra of the fruiting bodies of *P. ostreatus* harvested from the two growing substrates WS + SC (blue line) and D15 (orange line).

Apart from the bands due to ergothioneine, other bands can also be observed in the SERS spectra. The 1100–500 cm^{-1} region is practically empty of ergothioneine bands, and there appear two prominent bands at 659 and 734 cm^{-1} that can be assigned to ring breathing bands of the guanine and adenine. The bands at 865, 911, 965, and 1023 cm^{-1} can be assigned to the ribose-phosphate chain in nucleic acids, but with possible contributions from other specific fungi compounds such as chitin. Furthermore, the weak bands appearing at 1639, 1682, and 1693 cm^{-1} can be attributed to the amide I in proteins and also to ketonic C=O stretching. Finally, the presence of ester groups is evidenced by the presence of the weak band at 1769 cm^{-1}.

3.4.4. Polysaccharides

The ATR-FTIR spectra of polysaccharides extracted from the fruiting bodies are displayed in Figure 9. In both spectra, two small peaks are evident between 750–950 cm^{-1}, described as the signature bands for glucan [48]. The figure reveals a strong band in the region within 1200–1000 cm^{-1}, representing CO and CC stretching vibration. The two shoulders visible at 1037 and 1071 cm^{-1} can be attributed to glucans, as reported by Gomba et al. (2015) [49]. The strong peak that appears at 1642 cm^{-1} is assigned to Amide I in chitin but also to O-H-O bending of bound water in glucan, while that at 1535 cm^{-1} probably corresponds to Amide II vibration in chitin [49]. From the ATR-FTIR spectra is evident the band at 1398 cm^{-1}, which corresponds to the C-H stretching of the pyranose ring of chitin. Globally, the spectra of polysaccharides from mushrooms obtained on WS + SC and D15 are quite overlapping.

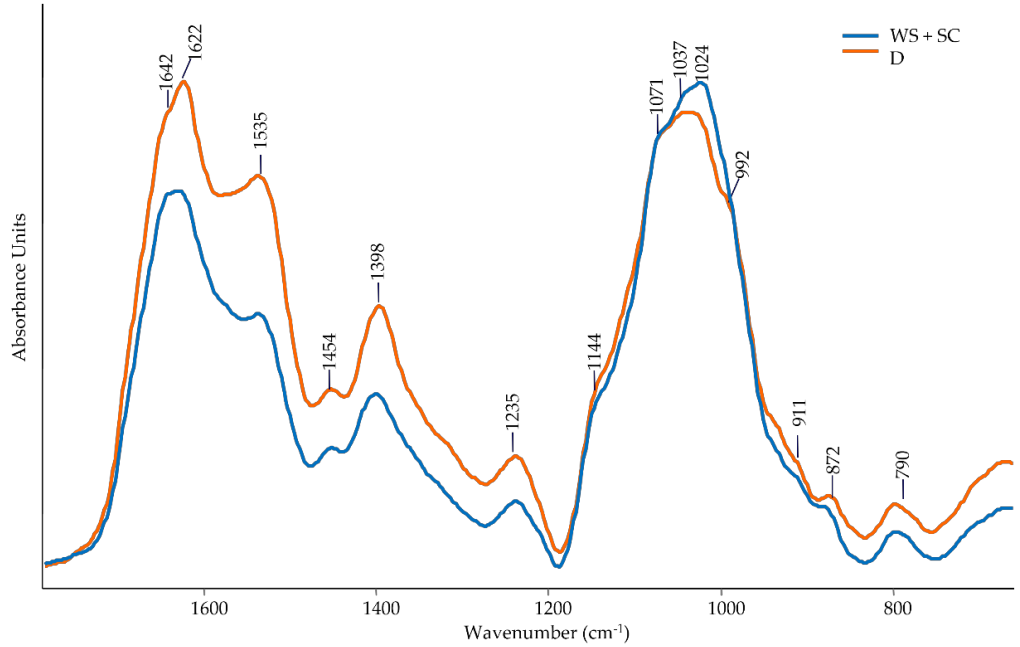

Figure 9. ATR-FTIR spectra (1800–700 cm^{-1}) of the polysaccharides extracted from fruiting bodies of *P. ostreatus* harvested from the two growing substrates WS + SC (blue line) and D15 (orange line).

4. Discussion

Anaerobic digestate, a by-product of biogas production, which was born as a sustainable industry, may become unsustainable if inadequate management occurs. All this has driven research toward different solutions to exploit it [13,18,50,51]. Similarly, mushroom farming is another developing industry thanks to the several promising properties of these organisms. Recent studies have focused on alternative and more sustainable growing substrates in terms of production and costs, and among these, digestate seems to provide good perspectives [24,40,52–56].

With this in mind, we tried to examine the relationship between the solid fraction of anaerobic digestate and *P. ostreatus* full-scale cultivation, using this agro-waste as an alternative or supplementary growing media. Chemical evaluations of matrices and mushrooms were carried out by using ATR-FTIR and SERS spectroscopies.

Preliminary structural evaluation of the matrices reveals that both WS + SC and D are rich in polysaccharides, such as cellulose and hemicellulose, and that is confirmed by the chemical analyses of the two substrates, which are quite similar regarding the organic carbon content, around 40% of the dry matter. C content is a fundamental factor for the optimal metabolism of fungi, and the ideal range is approximately 40% which is quite coincident with that of our matrices [20]. Moreover, the ATR-FTIR spectra show some characteristic bands linked to aromatic compounds, more evident in D, which can confirm the presence of lignin, as described by previous research [24,43].

At 1640 and 1550 cm^{-1}, we can find the amide groups; these two bands are more intense in D spectra, probably indicating a higher content in N-compounds, as also highlighted in the chemical evaluation. It has already been established that an optimal N availability can promote fungi growth [57,58]. As reported by Sozbir et al. (2015) [59] percentage between 1.94 and 2.08% seems to be an ideal range for *Pleurotus* spp. growth, rather than higher values which can be poisonous to its development [8]. Wan Mahari et al. (2020) [20] report that matrices with high nutritional values will promote the colonization process. Indeed, in this work, the higher nutrient composition of D, such as S, P, K, and Mg, compared to WS + SC, can better support mycelial growth. pH is one of the most important environmental factors that affect the enzyme activity in *Pleurotus* spp. [60]. The optimum pH established for mycelia growth was 5–6.5, which is that of the conventional substrate

used in this work; although D shows a pH of 9.05, it was previously described that higher values could encourage the development of mycelia rather than smaller values [8,20].

As a consequence of all the factors mentioned above and as previously analyzed by Fornito et al. (2020) [24], initial tests in Petri dishes confirm the capability of the selected strain of *P. ostreatus* (WH90) of colonizing in the same way the conventional substrate (WS + SC) and the experimental ones (D10, D20, D). From the growing curves, it is indeed apparent that the trend of mycelia development is comparable in conventional plates as well as in those added with D and with pure D; nonetheless, in the first phase, D stimulates faster mycelial colonization.

Despite the absence of statistical differences, AGR values corroborate these results. In fact, the average growth per day on the digestate matrix was more than 5 cm^2/d. The above findings are consistent with the work of Santi et al. (2015) [53], which demonstrated that *P. ostreatus* could proliferate on a digestate medium with positive results compared to wheat straw.

The consumption of N and C components is highlighted in the ATR-FTIR spectra registered after the cultivation. Indeed, variations in the lignin bands (1507, 1454, 1421 cm^{-1}) in WS + SC and in the amine bands (1550 cm^{-1}) in D, are emerged. The degradation of lignin may be verified through the reduction of the characteristic peaks at 1507 cm^{-1} and 1733 cm^{-1}. The colonization can be registered by looking at the increase at 1322 and 1643 cm^{-1}, which may correspond to the depolymerization of the lignocellulosic compounds as well as to residual mycelial protein groups. The resulting efficiency of mycelial colonization of both substrates is in line with the above and with previous findings presented by Fornito et al. (2020) [24] and Puliga et al. (2022) [23].

With these promising outcomes, we decided to proceed with full-scale cultivation in collaboration with the mushroom company. Considering it was the first trial and the availability of both WS and D, we decided to test a mixture of both as the experimental sample to evaluate the development of fruiting bodies. Interestingly, the production was almost the same with both substrates and even better with D, nearly 250 kg of fresh mushrooms. To strengthen our results, BE, resulting from the analyses, shows that at least half of the dry weight of both WS + SC and D15 was transformed into fruiting bodies. Again, with D15, results are distributed more homogeneously through the replicates. Overall, the production was perfectly comparable. However, D seems to stimulate a precocious development of mushrooms, as can be seen from P data. Previous research on *Agaricus* spp. has shown that P may depend on the type of growing matrix, as well as its formulation, texture, and environmental conditions [40,61].

In order to test the quality parameters, we compared chemical and spectroscopic analyses of mushrooms grown on the two matrices. The preliminary chemical evaluation reveals that the composition of macro and microelements is statistically equivalent, so the addition of D did not modify the nutrient content. Even more, nitrate and coliform bacteria values and agrochemical residues were not detectable, as well as heavy metals were below consented thresholds.

The structural analysis shows a predominance of carbohydrates which are generally known to represent more than 50% of the dry matter of mushrooms [3]. Besides, some medicinal and beneficial properties of fungi can be ascribed to the presence of some polysaccharides [62,63]. The spectra band at 1640 and 1544 cm^{-1} highlight the presence of N-compound, which means to a great extent, amino acids, proteins, and enzymes. These compounds can constitute up to 35% of the mushroom's dry matter and contribute to some of their fundamental characteristics [3]. Regarding the human diet, for instance, mushrooms provide a high amount of essential amino acids, among others, arginine, glutamic acid, aspartic acid, tryptophan, and lysine, which makes them a great alternative to animal products [3]. In addition, *Pleurotus* spp. has been studied for its remarkable production of lignocellulolytic enzymes that have a key role in the degradation of complex organic materials [64,65]. Some previous works have revealed that the growing substrate can emphasize the metabolites composition of the fruiting bodies [63]. Although further

studies are required to have a complete quality evaluation, this work provides a preliminary overview of the fruiting bodies derived from digestate and how their composition is perfectly comparable to that of mushrooms grown on conventional media.

An interesting method that can be used to better understand the molecular structure of the fruiting bodies is SERS spectroscopy. This technique allows better intercept of some vibrational signals, thus enhancing the identification of chemical compounds [30]. The resulting SERS spectra are dominated by the bands attributed to the amino acid ergothioneine [29]. This compound was ubiquitously found in plants and animals, and it is specifically very abundant in *P. ostreatus* [66]. This amino acid molecule was also detected in a previous work made by us on different mushrooms and displayed a high SERS activity, as also revealed by the Raman study in an analysis done on biological materials [30,67,68]. The characteristic band at 486 cm^{-1} can serve to identify it from other biomolecules that may occur in the same biological matrix. The high affinity of the S-containing five-member ring to the silver surface accounts for the high intensity of ergothioneine in SERS spectra. In addition, the high intensity of the ergothioneine SERS bands suggests that it could be exposed to the external part of the fungi because it is included in the fungi cell wall, although a possible breakdown of the fungal wall is not discharged. Despite the similarity of the SERS spectral profiles of fruiting bodies resulting from the two growing media, some variations can still be observed at 1324 and 1223 cm^{-1}. Since these bands are attributed to in-plane stretching motions of the imidazole thione ring, this difference could indicate a slight change in the orientation of this ring regarding the metal surface of Ag nanoparticles, according to the specific selection rules of SERS [31]. The appearance of intense bands of nucleic acids (DNA and RNA) between 600 and 900 cm^{-1} might be due to the disruption of the fungal membrane through the formation of holes in the fungal cell wall, as described elsewhere [69,70]. On the other hand, the strong intensity of the nucleic bases can be attributed to the high affinity of silver for purine and pyrimidine bases [71,72].

The analysis of polysaccharides reveals more details about mushroom composition. The most frequent compounds found are glucans, specifically two main types: branched (1→3)(1→6)-β-D-glucan and linear (1→3)-α-D-glucan. In ATR-FTIR spectra, these are visible at 790 and 872 cm^{-1}. The peak around 790 cm^{-1} is probably due to mannan [α(1-6) linked backbone with α(1-3) and α (1-2) linked branches], a type of glucan that is one component of fungal cell walls [46]. This finding agrees with the study of Baeva et al. (2020) [73], who defines the structure of several polysaccharide fractions of *P. ostreatus*. Numerous works have identified those compounds for their antioxidant and anti-inflammatory activity, thus enriching the mushroom's beneficial properties [62,63]. Usually combined with glucan, chitin is another important polysaccharide characteristic of the fungal cell wall structure. Its several biotechnological applications, among them pharmaceutical, nutraceutical, agricultural, and material science, make it a biopolymer of high interest [74,75]. From the spectra is evident the strong peak around 1398 cm^{-1} corresponds to C-H stretching of the pyranose ring of chitin; the two protein bands around 1630 and 1530 cm^{-1} can be useful as well to confirm the presence of chitin molecules [46,73,76]. The vibrational methods described above can be proposed as faster, non-destructive, and cheaper techniques to analyze some quality parameters of mushrooms.

5. Conclusions

In the last years, several studies have already confirmed the potential of mushroom cultivation as a valid tool to valorize different agro-wastes. Among these, anaerobic digestate, which is currently produced in large quantities, has proved to be an optimal substitute or supplement for conventional growing substrates. The quantity and quality of the fruiting body obtained in this work, using the substrate containing 15% of digestate, support the applicability of digestate in the industrial cultivation of *P. ostreatus*, which is the second most cultivated mushroom worldwide. The optimal composition of macro- and micronutrients, as well as the structural characteristics, have led to productivity comparable to that of the conventional substrate. In addition, qualitative parameters of the fruiting

bodies exhibit no differences. It is, therefore, possible to create a new chain of products with high added value and, at the same time, reduce the costs of raw materials.

Partnering with mushroom growers is a potential new business opportunity and an attractive new market for the biogas production sector. In our case study, we have shown that farms need to be located nearby to minimize transportation needs and GHG emissions and that providing zero-kilometer products can support local economies. On the other hand, from a wider perspective, the substitution of raw materials for agricultural waste benefits the sustainability of the production chain in agreement with circular economy criteria, providing a great impact for both the mushroom and biogas industries.

The future outlook is to recycle spent substrates for biogas plants on the basis of the European Commission's recent "REPowerEU" plan of 2022, which is aimed to gradually eliminate European dependence on Russian fossil resources and increase the resilience of the European Union's energy system.

Author Contributions: Conceptualization, V.Z. and F.P.; methodology, V.Z., F.P. and L.T.; formal analysis, V.Z.; investigation, V.Z., F.P. and L.T.; resources, O.F., A.Z. and S.S.-C.; data curation, V.Z. and F.P.; writing—original draft preparation, V.Z.; writing—review and editing, V.Z., F.P., A.Z., O.F. and S.S.-C.; visualization, V.Z. and L.T.; supervision, O.F., A.Z. and S.S.-C.; funding acquisition, O.F., A.Z. and S.S.-C. All authors have read and agreed to the published version of the manuscript.

Funding: This research was funded by Grant PON "Ricerca e Innovazione" 2014–2020, Ministero dell'Università e della Ricerca. This work was also financially supported by Ministerio de Ciencia e Innovación/FEDER funds (Project PID2020-113900RB-I00/AEI/10.13039/501100011033).

Data Availability Statement: The data presented in this study are available on request from the corresponding author.

Acknowledgments: We would like to thank Funghitex company (Latina, Italy) for giving us the opportunity to carry on the industrial cultivation process and the Mascetti-Sbardella farm (Latina, Italy) for providing us with corn digestate.

Conflicts of Interest: The authors declare no conflict of interest.

References

1. Lesa, K.N.; Khandaker, M.U.; Mohammad Rashed Iqbal, F.; Sharma, R.; Islam, F.; Mitra, S.; Emran, T.B. Nutritional Value, Medicinal Importance, and Health-Promoting Effects of Dietary Mushroom (*Pleurotus ostreatus*). *J. Food Qual.* **2022**, *2022*, 2454180. [CrossRef]
2. Papadaki, A.; Kachrimanidou, V.; Papanikolaou, S.; Philippoussis, A.; Diamantopoulou, P. Upgrading Grape Pomace through *Pleurotus* spp. Cultivation for the Production of Enzymes and Fruiting Bodies. *Microorganisms* **2019**, *7*, 207. [CrossRef]
3. Sharifi-Rad, J.; Butnariu, M.; Ezzat, S.M.; Adetunji, C.O.; Imran, M.; Sobhani, S.R.; Tufail, T.; Hosseinabadi, T.; Ramírez-Alarcón, K.; Martorell, M.; et al. Mushrooms-Rich Preparations on Wound Healing: From Nutritional to Medicinal Attributes. *Front. Pharmacol.* **2020**, *11*, 567518. [CrossRef]
4. Corrêa, R.C.G.; Brugnari, T.; Bracht, A.; Peralta, R.M.; Ferreira, I.C. Biotechnological, nutritional and therapeutic uses of *Pleurotus* spp. (Oyster mushroom) related with its chemical composition: A review on the past decade findings. *Trends Food Sci. Technol.* **2016**, *50*, 103–117. [CrossRef]
5. Feeney, M.J.; Miller, A.M.; Roupas, P. Mushrooms—Biologically Distinct and Nutritionally Unique: Exploring a "Third Food Kingdom". *Nutr. Today* **2014**, *49*, 301–307. [CrossRef]
6. FAOSTAT. Available online: https://www.fao.org/faostat/en/#home (accessed on 19 January 2023).
7. Giving Intelligence Teams an AI-Powered Advantage. Available online: https://www.reportlinker.com/ (accessed on 19 January 2023).
8. Bellettini, M.B.; Fiorda, F.A.; Maieves, H.A.; Teixeira, G.L.; Ávila, S.; Hornung, P.S.; Júnior, A.M.; Ribani, R.H. Factors Affecting Mushroom *Pleurotus* spp. *Saudi J. Biol. Sci.* **2019**, *26*, 633–646. [CrossRef]
9. Philippoussis, A.; Diamantopoulou, P. Agro-food industry wastes and agricultural residues convertion into high value products by mushroom cultivation. In Proceedings of the 7th International Conference on Mushroom Biology and Mushroom Products (ICMBMP7), Arcachon, France, 4–7 October 2011; pp. 4–7.
10. Kumla, J.; Suwannarach, N.; Sujarit, K.; Penkhrue, W.; Kakumyan, P.; Jatuwong, K.; Vadthanarat, S.; Lumyong, S. Cultivation of Mushrooms and Their Lignocellulolytic Enzyme Production through the Utilization of Agro-Industrial Waste. *Molecules* **2020**, *25*, 2811. [CrossRef] [PubMed]
11. Anwar, Z.; Gulfraz, M.; Irshad, M. Agro-Industrial Lignocellulosic Biomass a Key to Unlock the Future Bio-Energy: A Brief Review. *J. Radiat. Res. Appl. Sci.* **2014**, *7*, 163–173. [CrossRef]

12. Singh, N.B.; Chaudhary, R.G.; Desimone, M.F.; Agrawal, A.; Shukla, S.K. Green Synthesized Nanomaterials for Safe Technology in Sustainable Agriculture. *Curr. Pharm. Biotechnol.* **2023**, *24*, 61–85. [CrossRef]
13. Monlau, F.; Sambusiti, C.; Ficara, E.; Aboulkas, A.; Barakat, A.; Carrère, H. New Opportunities for Agricultural Digestate Valorization: Current Situation and Perspectives. *Energy Environ. Sci.* **2015**, *8*, 2600–2621. [CrossRef]
14. European Commission and Industry Leaders Launch Biomethane Industrial Partnership to Support the 35 Bcm Target on Biomethane by 2030 European Biogas Association. Available online: https://www.europeanbiogas.eu/european-commission-and-industry-leaders-launch-biomethane-industrial-partnership-to-support-the-35-bcm-target-on-biomethane-by-2030/ (accessed on 20 February 2023).
15. Corden, C.; Bougas, K.; Cunningham, E.; Tyrer, D.; Kreißig, J.; Zetti, E.; Gamero, E.; Wildey, R.; Crookes, M. Digestate and Compost as Fertilisers: Risk Assessment and Risk Management Options. Wood Environment & Infrastructure Solutions UK Limited. (Doc Ref. 40039CL003i3). 2019. Available online: https://ec.europa.eu/environment/chemicals/reach/pdf/40039%20Digestate%20and%20Compost%20RMOA%20-%20Final%20report%20i2_20190208.pdf (accessed on 20 March 2023).
16. Gioelli, F.; Dinuccio, E.; Balsari, P. Residual Biogas Potential from the Storage Tanks of Non-Separated Digestate and Digested Liquid Fraction. *Bioresour. Technol.* **2011**, *102*, 10248–10251. [CrossRef] [PubMed]
17. Menardo, S.; Gioelli, F.; Balsari, P. The Methane Yield of Digestate: Effect of Organic Loading Rate, Hydraulic Retention Time, and Plant Feeding. *Bioresour. Technol.* **2011**, *102*, 2348–2351. [CrossRef] [PubMed]
18. Dahlin, J.; Herbes, C.; Nelles, M. Biogas Digestate Marketing: Qualitative Insights into the Supply Side. *Resour. Conserv. Recycl.* **2015**, *104*, 152–161. [CrossRef]
19. Phan, C.-W.; Sabaratnam, V. Potential Uses of Spent Mushroom Substrate and Its Associated Lignocellulosic Enzymes. *Appl. Microbiol. Biotechnol.* **2012**, *96*, 863–873. [CrossRef] [PubMed]
20. Wan Mahari, W.A.; Peng, W.; Nam, W.L.; Yang, H.; Lee, X.Y.; Lee, Y.K.; Liew, R.K.; Ma, N.L.; Mohammad, A.; Sonne, C.; et al. A Review on Valorization of Oyster Mushroom and Waste Generated in the Mushroom Cultivation Industry. *J. Hazard. Mater.* **2020**, *400*, 123156. [CrossRef]
21. Sánchez, C. Lignocellulosic Residues: Biodegradation and Bioconversion by Fungi. *Biotechnol. Adv.* **2009**, *27*, 185–194. [CrossRef]
22. Philippoussis, A.; Zervakis, G.; Diamantopoulou, P. Bioconversion of Agricultural Lignocellulosic Wastes through the Cultivation of the Edible Mushrooms *Agrocybe aegerita*, *Volvariella volvacea* and *Pleurotus* spp. *World J. Microbiol. Biotechnol.* **2001**, *17*, 191–200. [CrossRef]
23. Puliga, F.; Leonardi, P.; Minutella, F.; Zambonelli, A.; Francioso, O. Valorization of Hazelnut Shells as Growing Substrate for Edible and Medicinal Mushrooms. *Horticulturae* **2022**, *8*, 214. [CrossRef]
24. Fornito, S.; Puliga, F.; Leonardi, P.; Di Foggia, M.; Zambonelli, A.; Francioso, O. Degradative Ability of Mushrooms Cultivated on Corn Silage Digestate. *Molecules* **2020**, *25*, 3020. [CrossRef]
25. Hultberg, M.; Asp, H.; Bergstrand, K.J.; Golovko, O. Production of Oyster Mushroom (*Pleurotus ostreatus*) on Sawdust Supplemented with Anaerobic Digestate. *Waste Manag.* **2023**, *155*, 1–7. [CrossRef]
26. Movasaghi, Z.; Rehman, S.; ur Rehman, D.I. Fourier Transform Infrared (FTIR) Spectroscopy of Biological Tissues. *Appl. Spectrosc. Rev.* **2008**, *43*, 134–179. [CrossRef]
27. Meenu, M.; Xu, B. Application of Vibrational Spectroscopy for Classification, Authentication and Quality Analysis of Mushroom: A Concise Review. *Food Chem.* **2019**, *289*, 545–557. [CrossRef] [PubMed]
28. Dina, N.E.; Gherman, A.M.R.; Chiş, V.; Sârbu, C.; Wieser, A.; Bauer, D.; Haisch, C. Characterization of Clinically Relevant Fungi via SERS Fingerprinting Assisted by Novel Chemometric Models. *Anal. Chem.* **2018**, *90*, 2484–2492. [CrossRef] [PubMed]
29. Fornasaro, S.; Gurian, E.; Pagarin, S.; Genova, E.; Stocco, G.; Decorti, G.; Sergo, V.; Bonifacio, A. Ergothioneine, a Dietary Amino Acid with a High Relevance for the Interpretation of Label-Free Surface Enhanced Raman Scattering (SERS) Spectra of Many Biological Samples. *Spectrochim. Acta Part A Mol. Biomol. Spectrosc.* **2021**, *246*, 119024. [CrossRef]
30. Puliga, F.; Zuffi, V.; Zambonelli, A.; Francioso, O.; Sanchez-Cortes, S. Spectroscopic Analysis of Mushrooms by Surface-Enhanced Raman Scattering (SERS). *Chem. Biol. Technol. Agric.* **2022**, *9*, 100. [CrossRef]
31. Aroca, R. *Surface Enhanced Vibrational Spectroscopy*; Wiley: Hoboken, NJ, USA, 2006; ISBN 978-0-471-60731-1.
32. Aroca, R.F. Plasmon enhanced spectroscopy. *Phys. Chem. Chem. Phys.* **2013**, *15*, 5355–5363. [CrossRef] [PubMed]
33. Butler, H.J.; Ashton, L.; Bird, B.; Cinque, G.; Curtis, K.; Dorney, J.; Esmonde-White, K.; Fullwood, N.J.; Gardner, B.; Martin-Hirsch, P.L.; et al. Using Raman spectroscopy to characterize biological materials. *Nat. Protoc.* **2016**, *11*, 664–687. [CrossRef]
34. Le Ru, E.; Etchegoin, P. *Principles of Surface Enhanced Raman Spectroscopy (and Related Plasmonic Effects)*; Elsevier: Amsterdam, The Netherlands, 2009.
35. Moskovits, M. Surface-enhanced spectroscopy. *Rev. Mod. Phys.* **1985**, *57*, 783–826. [CrossRef]
36. Moskovits, M.; Suh, J.S. Surface selection rules for surface-enhanced Raman spectroscopy: Calculations and application to the surface-enhanced Raman spectrum of phthalazine on silver. *J. Phys. Chem.* **1984**, *88*, 5526–5530. [CrossRef]
37. Tryfinopoulou, P.; Chourdaki, A.; Nychas, G.-J.E.; Panagou, E.Z. Competitive Yeast Action against *Aspergillus carbonarius* Growth and Ochratoxin A Production. *Int. J. Food Microbiol.* **2020**, *317*, 108460. [CrossRef]
38. Sinclair, C.G.; Cantero, D. Fermentation modelling. In *Fermentation a Practical Approach*; McNeil, B.L., Harvey, M., Eds.; IRL Press: New York, NY, USA, 1989; pp. 65–112. ISBN 978-0-19-963044-8.
39. Oei, P. *Mushroom Cultivation: Appropriate Technology for Mushroom Growers*, 3rd ed.; Backhuys: Leiden, The Netherlands, 2003; ISBN 978-90-5782-137-0.

40. Jasińska, A.; Dawidowicz, L.; Siwulski, M.; Kilinowski, P. Growth of Mycelium of Different Edible and Medicinal Mushrooms on Medium Supplemented with Digestate from AD Biogas Plant. *Not. Bot. Horti. Agrobo.* **2017**, *45*, 498–506. [CrossRef]
41. Cocchi, L.; Vescovi, L.; Petrini, L.E.; Petrini, O. Heavy metals in edible mushrooms in Italy. *Food Chem.* **2006**, *98*, 277–284. [CrossRef]
42. Leopold, N.; Lendl, B. A New Method for Fast Preparation of Highly Surface-Enhanced Raman Scattering (SERS) Active Silver Colloids at Room Temperature by Reduction of Silver Nitrate with Hydroxylamine Hydrochloride. *J. Phys. Chem. B* **2003**, *107*, 5723–5727. [CrossRef]
43. Liu, R.; Yu, H.; Huang, Y. Structure and Morphology of Cellulose in Wheat Straw. *Cellulose* **2005**, *12*, 25–34. [CrossRef]
44. Gao, A.H.; Bule, M.V.; Laskar, D.D.; Chen, S. Structural and Thermal Characterization of Wheat Straw Pretreated with Aqueous Ammonia Soaking. *J. Agric. Food Chem.* **2012**, *60*, 8632–8639. [CrossRef] [PubMed]
45. Provenzano, M.R.; Iannuzzi, G.; Fabbri, C.; Senesi, N. Qualitative Characterization and Differentiation of Digestates from Different Biowastes Using FTIR and Fluorescence Spectroscopies. *JEP* **2011**, *02*, 83–89. [CrossRef]
46. Das, B.; Rajkonwar, J.; Jagannath, A.; Raul, P.K.; Deb, U. Infra Red Spectra of Different Species of Cultivated Oyster Mushrooms Possible Tool for Identifying Bioactive Compounds and Establishing Taxonomic Linkage. *Def. Life Sci. J.* **2020**, *5*, 118–124. [CrossRef]
47. Zervakis, G.I.; Bekiaris, G.; Tarantilis, P.A.; Pappas, C.S. Rapid Strain Classification and Taxa Delimitation within the Edible Mushroom Genus Pleurotus through the Use of Diffuse Reflectance Infrared Fourier Transform (DRIFT) Spectroscopy. *Fungal Biol.* **2012**, *116*, 715–728. [CrossRef]
48. Synytsya, A.; Novak, M. Structural analysis of glucans. *Ann. Transl. Med.* **2014**, *2*, 17. [CrossRef]
49. Gomba, G.K.; Synytsya, A.; Švecová, P.; Coimbra, M.A.; Čopíková, J. Distinction of Fungal Polysaccharides by N/C Ratio and Mid Infrared Spectroscopy. *Int. J. Biol. Macromol.* **2015**, *80*, 271–281. [CrossRef]
50. Sheets, J.P.; Yang, L.; Ge, X.; Wang, Z.; Li, Y. Beyond Land Application: Emerging Technologies for the Treatment and Reuse of Anaerobically Digested Agricultural and Food Waste. *Waste Manag.* **2015**, *44*, 94–115. [CrossRef] [PubMed]
51. Udayasimha, D.L.; Vijayalakshmi, Y.C. Sustainable Waste Managementby Growing Mushroom (*Pleurotus florida*) on Anaerobically Digested Waste and Agro Residues. *Int. J. Eng. Res.* **2012**, *1*, 1–8.
52. O'Brien, B.J.; Milligan, E.; Carver, J.; Roy, E.D. Integrating Anaerobic Co-Digestion of Dairy Manure and Food Waste with Cultivation of Edible Mushrooms for Nutrient Recovery. *Bioresour. Technol.* **2019**, *285*, 121312. [CrossRef] [PubMed]
53. Santi, G.; Muzzini, V.G.; Galli, E.; Proietti, S.; Moscatello, S.; Battistelli, A. Mycelial growth and enzymatic activities of white-rot fungi on anaerobic digestates from industrial biogas plants. *Environ. Eng. Manag. J.* **2015**, *14*, 1713–1719. [CrossRef]
54. Singh, S.; Harms, H.; Schlosser, D. Screening of Ecologically Diverse Fungi for Their Potential to Pretreat Lignocellulosic Bioenergy Feedstock. *Appl. Microbiol. Biotechnol.* **2014**, *98*, 3355–3370. [CrossRef]
55. Schimpf, U.; Schrader, A.; Hübner, A.; Schulz, R.; Neubauer, P. Utilisation of Solid Digestate from Acidification Reactors of Continues Two-Stage Anaerobic Digestion Processes in *Lentinula edodes* Cultivation. *Bioresour. Technol. Rep.* **2019**, *8*, 100322. [CrossRef]
56. Zhou, J.-L.; Song, S.; Huang, Z.-X.; Yang, L.; Jiao, A.-G.; Liu, Y.; Wang, S.-X. Cultivation of *Pleurotus ostreatus*, a Potential Candidate for Biogas Residues Degradation. *BioRes* **2018**, *13*, 5432–5449. [CrossRef]
57. Hoa, H.T.; Wang, C.-L.; Wang, C.-H. The Effects of Different Substrates on the Growth, Yield, and Nutritional Composition of Two Oyster Mushrooms (*Pleurotus ostreatus* and *Pleurotus cystidiosus*). *Mycobiology* **2015**, *43*, 423–434. [CrossRef]
58. Osunde, M.O.; Olayinka, A.; Fashina, C.D.; Torimiro, N. Effect of Carbon-Nitrogen Ratios of Lignocellulosic Substrates on the Yield of Mushroom (*Pleurotus pulmonarius*). *OALib* **2019**, *6*, 1–8. [CrossRef]
59. Sözbir, G.D.; Bektas, I.; Zulkadir, A. Lignocellulosic Wastes Used for the Cultivation of *Pleurotus ostreatus* Mushrooms: Effects on Productivity. *BioResources* **2015**, *10*, 4686–4693. [CrossRef]
60. Sardar, H.; Ali, M.A.; Ayyub, C.M.; Ahmad, R. Effects of different culture media, temperature and pH levels on the growth of wild and exotic *Pleurotus* species. *Pak. J. Phytopathol.* **2015**, *27*, 139–145.
61. Zied, D.C.; Minhoni, M.T.A.; Kopytowski-Filho, J.; Andrade, M.C.N. Production of *Agaricus blazei* Ss. Heinemann (*A. brasiliensis*) on Different Casing Layers and Environments. *World J. Microbiol. Biotechnol.* **2010**, *26*, 1857–1863. [CrossRef]
62. Berger, R.G.; Bordewick, S.; Krahe, N.-K.; Ersoy, F. Mycelium vs. Fruiting Bodies of Edible Fungi—A Comparison of Metabolites. *Microorganisms* **2022**, *10*, 1379. [CrossRef] [PubMed]
63. Zhang, Y.; Dai, L.; Kong, X.; Chen, L. Characterization and in Vitro Antioxidant Activities of Polysaccharides from *Pleurotus ostreatus*. *Int. J. Biol. Macromol.* **2012**, *51*, 259–265. [CrossRef] [PubMed]
64. Kurt, S.; Buyukalaca, S. Yield Performances and Changes in Enzyme Activities of *Pleurotus* spp. (*P. ostreatus* and *P. sajor-caju*) Cultivated on Different Agricultural Wastes. *Bioresour. Technol.* **2010**, *101*, 3164–3169. [CrossRef] [PubMed]
65. Pérez-Chávez, A.M.; Alberti, M.M.; Albertó, E. Evaluation of Ligninolytic Activity in Spent Mushroom Substrate from Four Cultivated Mushrooms. *J. Bioresour. Bioprod.* **2022**, *7*, 288–294. [CrossRef]
66. Pang, L.; Wang, T.; Liao, Q.; Cheng, Y.; Wang, D.; Li, J.; Fu, C.; Zhang, C.; Zhang, J. Protective Role of Ergothioneine Isolated from *Pleurotus ostreatus* against Dextran Sulfate Sodium-Induced Ulcerative Colitis in Rat Model. *J. Food Sci.* **2022**, *87*, 415–426. [CrossRef]

67. Witkowska, E.; Jagielski, T.; Kamińska, A.; Kowalska, A.; Hryncewicz-Gwóźdź, A.; Waluk, J. Detection and Identification of Human Fungal Pathogens Using Surface-Enhanced Raman Spectroscopy and Principal Component Analysis. *Anal. Methods* **2016**, *8*, 8427–8434. [CrossRef]
68. Feng, S.; Lin, J.; Cheng, M.; Li, Y.-Z.; Chen, G.; Huang, Z.; Yu, Y.; Chen, R.; Zeng, H. Gold Nanoparticle Based Surface-Enhanced Raman Scattering Spectroscopy of Cancerous and Normal Nasopharyngeal Tissues under Near-Infrared Laser Excitation. *Appl. Spectrosc.* **2009**, *63*, 1089–1094. [CrossRef]
69. Kim, J.S.; Kuk, E.; Yu, K.N.; Kim, J.-H.; Park, S.J.; Lee, H.J.; Kim, S.H.; Park, Y.K.; Park, Y.H.; Hwang, C.-Y.; et al. Antimicrobial Effects of Silver Nanoparticles. *Nanomed. Nanotechnol. Biol. Med.* **2007**, *3*, 95–101. [CrossRef]
70. Kim, J.; Lee, J.; Kwon, S.; Jeong, S. Preparation of Biodegradable Polymer/Silver Nanoparticles Composite and Its Antibacterial Efficacy. *J. Nanosci. Nanotechnol.* **2009**, *9*, 1098–1102. [CrossRef] [PubMed]
71. Otto, C.; van den Tweel, T.J.J.; de Mul, F.F.M.; Greve, J. Surface-Enhanced Raman Spectroscopy of DNA Bases. *J. Raman Spectrosc.* **1986**, *17*, 289–298. [CrossRef]
72. Rivas, L.; Murza, A.; Sánchez-Cortés, S.; García-Ramos, J.V. Interaction of Antimalarial Drug Quinacrine with Nucleic Acids of Variable Sequence Studied by Spectroscopic Methods. *J. Biomol. Struct. Dyn.* **2000**, *18*, 371–383. [CrossRef]
73. Baeva, E.; Bleha, R.; Sedliaková, M.; Sushytskyi, L.; Švec, I.; Čopíková, J.; Jablonsky, I.; Klouček, P.; Synytsya, A. Evaluation of the Cultivated Mushroom *Pleurotus ostreatus* Basidiocarps Using Vibration Spectroscopy and Chemometrics. *Appl. Sci.* **2020**, *10*, 8156. [CrossRef]
74. Joseph, S.M.; Krishnamoorthy, S.; Paranthaman, R.; Moses, J.A.; Anandharamakrishnan, C. A Review on Source-Specific Chemistry, Functionality, and Applications of Chitin and Chitosan. *Carbohydr. Polym. Technol. Appl.* **2021**, *2*, 100036. [CrossRef]
75. Harish Prashanth, K.V.; Tharanathan, R.N. Chitin/Chitosan: Modifications and Their Unlimited Application Potential—An Overview. *Trends Food Sci. Technol.* **2007**, *18*, 117–131. [CrossRef]
76. Boureghda, Y.; Satha, H.; Bendebane, F. Chitin–Glucan Complex from *Pleurotus ostreatus* Mushroom: Physicochemical Characterization and Comparison of Extraction Methods. *Waste Biomass Valor.* **2021**, *12*, 6139–6153. [CrossRef]